Assessment of Radiological Hazards of Sedimentary, Igneous and Sediments Natural Rocks

Wafaa Arafa[1], Hala Mahmoud[1], Eman Yousf[2], Ashry Ashry[3], Ibrahim Elaassy[2], Ahmed Elsersy[4]

[1]Faculty of Women, Ain Shams University, Cairo, Egypt
[2]Nuclear Material Authority, Cairo, Egypt
[3]Faculty of Education, Ain Shams University, Cairo, Egypt
[4]National Institute of Standard, Giza, Egypt
Email: hsamman@aucegypt.edu

Abstract

Gamma-ray spectroscopy based on a 100% efficiency hyper-pure germanium detector was used to evaluate the activity concentrations of ^{226}Ra, ^{232}Th, and ^{40}K natural radionuclides in sedimentary, conglomerate, igneous and sediments rock samples collected from four different locations in Eastern desert in Egypt. The obtained activity concentrations are used to evaluate the radiological hazards indices, absorbed dose rate, annual effective dose equivalent in air, radium equivalent, external and internal hazard index, radiation level index, annual gonadal dose equivalent, excess lifetime cancer risk and exposure rate. The results show that 1) the absorbed dose rate depends on the rock type, 2) the annual effective dose equivalent in air in 71% of sample below 20 mSvy^{-1} (permissible limit for workers), 3) the conglomerate rocks show low radioactivity level, 4) sedimentary rocks are rich in radium while igneous rocks are rich in thorium and the sediments rocks are rich in both radium and thorium.

1. Introduction

Naturally occurring radioactive elements like uranium (^{238}U), thorium (^{232}Th), and potassium (^{40}K), along with their decay by-products such as radium (^{226}Ra) and radon (^{220,222}Rn), are examples of NORM. These elements have always been

present in the Earth's crust and atmosphere and their concentrations may vary from one place such as places near mining activities to another. The designation of NORM serves the purpose of delineating "natural radioactivity" from anthropogenic sources of radioactive material, such as those utilized in nuclear medicine and in industry [1]. These radionuclides have different sources, including the earth's crust, rocks, soils, plants, water, sediments, minerals, and air [2].

Uranium, thorium, and potassium-40 are significant sources of radiation, which can be found in various types of rocks, particularly in igneous and sedimentary rocks. All building materials are mostly composed of rock and soil containing ^{238}U and ^{232}Th decay series and ^{40}K. These natural radionuclides may cause both external exposure due to their direct gamma radiation and internal exposure from radon gas. If inhaled for an extended period, alpha particles can become trapped in the lungs, causing irritation to the cells of mucous membranes, and potentially leading to a high risk of lung cancer. There has been increased trend of public worldwide in using ceramic tile, stone, marble, granite, etc., due to their polished surface, decorative and different attractive colours, as building materials. The ceramic tiles are generally made of a mixture of different raw materials including clays, quartz materials and feldspar. The marble, on the other hand, is a metamorphic rock composed of recrystallized carbonate minerals. It is extracted from the mountains and after mining it is transported to marble factories in various cities. Granite is the best-known igneous rock. It is composed mainly of quartz and feldspar with minor amounts of mica, amphiboles, and other minerals. A common opacifying constituent of glazes, applied to these materials, is zircon that may cause natural radioactivity concentration significantly higher than the average values for building materials. Hazard parameters, play a significant role to assess the potential radiation hazards posed by these building materials [3].

Workers engaged in anthropogenic activities, particularly in mining, face a significant risk of radiation exposure from Naturally Occurring Radioactive Materials (NORM). These materials are often present in various geological formations and can be released into the environment during mining processes, leaving behind contamination that poses potential health hazards. Without proper monitoring and containment measures, the environment can become laden with substances that emit radiation, presenting remote but significant risks to both workers and surrounding communities. Effective management strategies are imperative to mitigate these risks and ensure the safety of those involved in anthropogenic activities [4].

Radium (^{226}Ra) nuclide is commonly chosen in studies due to its gamma rays emitted by its two main daughters, ^{214}Pb and ^{214}Bi. These gamma rays contribute to 98% of the external dose from all nuclides in the ^{238}U series. It is crucial to determine the baseline of natural radiation and radioactivity so that man-made contamination can be contrasted with natural radioactivity. This makes it possible to detect contamination instantly, and thus appropriate measures against the risk to human health and the environment from radiation can be taken. For the

above reasons, the worldwide interest in natural radiation exposure has received particular attention and has led to extensive surveys in many countries. This reflects the activity concentration of primordial radionuclides in the soil. Approximately 95% of the world's population is assumed to live in areas of normal background radiation, with outdoor exposure ranging from 24 to 160 nGy·h^{-1} [5]. Thus, environmental studies to determine the levels of radiation from natural sources are very important. The external absorbed dose rate in air at 1 m above ground level and the annual effective dose are commonly used to estimate exposure to the population. Knowledge of radionuclide distribution is needed to understand natural environmental radioactivity and the associated external exposure resulting from gamma radiation, which varies based on geological and geographical conditions.

The present study could serve as baseline data for populated areas near the studied locations, with the aim of assessing the risk caused to workers engaged in anthropogenic activities, particularly in mining by outdoor exposure to terrestrial radiation, in addition to guiding decision-makers in solving some natural environmental problems that may be found anywhere in the world. Therefore, data obtained from such studies may be used locally to establish whether and where controls are needed. Furthermore, the results would enrich the world's data bank, which is important for evaluating the worldwide average values of radiometric and dosimetry quantities.

The goal of the current study is to measure the naturally occurring radioactivity levels of radium-226, thorium-232, and potassium-40 in rocks some (sedimentary, conglomerate, igneous, and sediments) samples collected from four various sites in Eastern desert in Egypt. The study was conducted by using an advanced gamma spectrometer using 100% HPGe detector. The obtained information might be valuable for environmental radiation protection studies and can be used to estimate population (workers) exposure to radiation. The study evaluate and compare the absorbed dose rates D (nGy·h^{-1}) and associated radiological effect indices such as Annual Effective Dose Equivalent *AEDE* (mSv·y^{-1}), Radium Equivalent Activity Ra_{eq} (Bq·kg^{-1}), Internal and External Hazard Index (H_{ex} and H_{in}), Radiation Level Index (I_γ), Annual Gonad Dose Equivalent *AGDE* (μSv·y^{-1}), Excess lifetime cancer risk *ELCR* (mSv·y^{-1}) and Exposure rate *ER* (μRh^{-1}) with published average values and accepted limits to assess the level of natural radioactivity and the associated radiological hazards to human health. In this work only the hazards due external exposure will be considered since the occupancy of such remote area is limited to the workers who might be present.

2. Materials and Methods

2.1. Sample Collection and Preparation

Twenty-one samples were collected according to its type from four different locations in Eastern desert in Egypt. This study includes ten samples of sedimentary, two of conglomerate, seven of igneous and two of sediments rocks.

The collected samples were dried at 105˚C temperature for 24 hours to eliminate the moisture content. Then crushed and sieved through 200 mesh size. The samples were weighted and placed in polyethylene beaker of 250 cm³ volume. The beakers were completely sealed for one month to allow secular equilibrium between ^{222}Rn and its daughters.

2.2. Sample Counting

In the present study, the used gamma-ray spectrometer consists of 100% relative efficiency n-type hyper pure germanium detector (HPGe) connected to X-cooler-III electric cooling system. The X-cooler cooling system is used to assure permanent cooling facility of the detector. The detector is surrounded by 10 cm thickness of reprocessed high-performance and low-background lead shield cylinder. A graded liner of copper and tin layers is provided for the suppression of lead x-rays. The detection range is between 10 keV and 10 MeV. The detector has a resolution (FWHM) of 1.9 at 1332 keV γ-ray line of ^{60}Co. The detector is connected to digital spectrometer DSPC-pro which has high voltage, advanced spectroscopy amplifier and 16 k multichannel analyser. The acquisition system and analysis of spectra are controlled by gamma-Vision software [6]. The energy and efficiency calibration were performed using standard soil matrix source [7]. Angle-3 software was used to generate efficiency curves corrected for volume and density which ranged between 0.6 and 2.6 g·cm⁻³ [8]. The high activity samples were counted during a period of 6 hours (live time) while, the low activity samples were counted for 24 hours live time. The environmental gamma-rays background at the laboratory site has been determined using an empty container that is counted in the same condition as the samples. The analysis of the collected samples has been carried out using Gamma Vision software [6]. The obtained data have been corrected for density and self-absorption effect of gamma ray, which depends on the density of the sample [9].

2.3. Calculation of Radionuclides Concentration

The activity concentration (*A*) in Bq·kg⁻¹ of each radionuclide in the samples was determined by using Equation (1).

$$A = \frac{CPS}{W * I * \varepsilon} \tag{1}$$

where *CPS* is the net gamma counts per second corrected for background, *W* is the dry mass of the sample (kg), *I* is the absolute transition probability of gamma-ray and ε is the detector efficiency at energy *E* [10].

2.4. Radiological Hazard Indices

2.4.1. Absorbed Dose Rate *D*

A direct connection between radioactivity concentrations of natural radionuclides and their exposure is known as the absorbed dose rate in the air at 1 meter above the ground surface. The mean activity concentrations of ^{226}Ra, ^{232}Th, and

^{40}K (Bq·kg^{-1}) in the studied samples are used to calculate the absorbed dose rate using Equation (2)

$$D\left(\mathrm{nGy} \cdot \mathrm{h}^{-1}\right) = 0.462 A_{Ra} + 0.604 A_{Th} + 0.0417 A_{K} \tag{2}$$

where D is the absorbed dose rate in nGy·h^{-1}, A_{Ra}, A_{Th} and A_{K} are the activity concentration of ^{226}Ra, ^{232}Th and ^{40}K, respectively [11] [12].

2.4.2. Annual Effective Dose Equivalent (*AEDE*)

The absorbed dose rate in air at 1 meter above the ground surface does not directly provide the radiological risk to which an individual is exposed. The absorbed dose can be considered in terms of the annual effective dose equivalent from indoor terrestrial gamma radiation which is converted from the absorbed dose by considering two factors, namely the conversion coefficient from absorbed dose in air to effective dose (0.7 Sv·Gy^{-1}) and the outdoor occupancy factor (0.2). The annual effective dose equivalent can be estimated using the following equation.

$$AEDE\left(\mathrm{mSv} \cdot \mathrm{y}^{-1}\right) = D\left(\mathrm{nGy} \cdot \mathrm{h}^{-1}\right) \times 0.2 \times 0.7\left(\mathrm{Sv} \cdot \mathrm{Gy}^{-1}\right) \times 10^{-6} \tag{3}$$

2.4.3. Radium Equivalent Activity (*Ra$_{eq}$*)

A common radiological index referred to radium equivalent was used in this study to evaluate the actual activity level of ^{226}Ra, ^{232}Th and ^{40}K in the samples and the radiation hazards associated with these radionuclides. This is as results of the fact that distribution of natural radionuclide in the samples under investigation is not uniform and is assumed that 370 Bq·kg^{-1} of Ra, 259 Bq·kg^{-1} of Th and 4810 Bq·kg^{-1} of K produce an equal gamma-ray dose. This index is usually known as radium equivalent activity [13] and given by Equation (4).

$$Ra_{eq} = A_{Ra} + 1.34 A_{Th} + 0.077 A_{Th} \tag{4}$$

2.4.4. Internal and External Hazard Index (*H$_{ex}$* and *H$_{in}$*)

The existence of natural radionuclides causes the emission of γ-ray in the environment. The internal hazard index (H_{in}) and the external hazard index (H_{ex}) are used to estimate the biological hazard of the natural gamma radiation [14]. Internal radiation explained as the radiation which occurs if a human consuming something that emits radiation, and then the radiation entered and radiated to the human's body directly and resulted in radiological hazards. The internal hazard index, H_{in} is given by Equation (5).

$$H_{in} = \frac{A_{Ra}}{185} + \frac{A_{Th}}{259} + \frac{A_{K}}{4810} \tag{5}$$

where A_{Ra}, A_{Th} and A_{K} are defined in Equation (2). For the safe use as building materials H_{in} should be less than unity [15].

External radiation exposure due to ^{226}Ra, ^{232}Th and ^{40}K is external assessed by external hazard index, H_{ex} [16]. Its level is calculated by the Equation (6)

$$H_{ex} = \frac{A_{Ra}}{370} + \frac{A_{Th}}{259} + \frac{A_{K}}{4810} \tag{6}$$

For the safe use of samples, Hex should be less than unity [17].

2.4.5. Radiation Level Index (I_γ)

This index can be used to estimate the level of γ-radiation hazard associated with the natural radionuclides is given by Equation (7).

$$I_\gamma = \frac{A_{Ra}}{150} + \frac{A_{Th}}{100} + \frac{A_K}{1500} \tag{7}$$

For the safe use of samples, I_γ should be less than unity [18].

2.4.6. Annual Gonadal Dose Equivalent

The bone marrow and bone surface cells are considered as organs of interest therefore, the Annual Gonadal Dose Equivalent (*AGDE*) was introduced to take care of the specific activities arising from ^{226}Ra, ^{232}Th and ^{40}K. The *AGDE* was calculated using Equation (8) [1].

$$AGDE\left(\text{mSv}\cdot\text{y}^{-1}\right) = 3.09 A_{Ra} + 4.18 A_{Th} + 0.31 A_K \tag{8}$$

2.4.7. Excess Lifetime Cancer Risk (*ELCR*)

The excess lifetime cancer risk (*ELCR*) for outdoor exposure, gives the probability for an individual to develop cancer over a lifetime at a given exposure. This was calculated using Equation (9).

$$ELCR\left(\text{mSv}\cdot\text{y}^{-1}\right) = AEDE \times LE \times RF \tag{9}$$

where *AGDE* is the annual effective dose equivalent, *LE* life expectancy (66 years) and *RF* is risk factor (Sv^{-1}), which is 0.05 [19]

2.4.8. Exposure Rate (*ER*)

The exposure rate was calculated using Equation (10) [20]

$$ER\left(\mu\text{Rh}^{-1}\right) = 1.9 A_{Ra} + 2.28 A_{Th} + 0.314 A_K \tag{10}$$

3. Results and Discussion

Activity Concentrations

Table 1 presents the activity concentration of natural radionuclides ^{226}Ra, ^{232}Th, and ^{40}K in samples collected from various locations under investigation. Additionally, it includes the mean values of these radionuclides' activity concentrations in samples categorized into Sedimentary, Conglomerate, Igneous, and Sediments groups of rocks. Previous studies conducted in Egypt and from the international literature are also included in this table for comparison purpose. Such comparisons offer valuable insights into variations and similarities in natural radioactivity levels across various geological formations and geographical regions, contributing to a comprehensive understanding of radiation exposure risks associated with specific rock types and locations.

However, the concentrations of ^{226}Ra, ^{232}Th, and ^{40}K obtained in the present work are comparable to those published by [21] in pegmatites rocks in other locations in the Egyptian desert. Nevertheless, they are significantly higher com-

pared to the activity concentration of some commercial Egyptian granite samples used as a building material and published by reference [22].

The mean activity concentrations of ^{226}Ra, ^{232}Th, and ^{40}K in sedimentary, igneous, and sediment samples obtained in the present work, as well as the mean activity concentration of pegmatite rock samples [21] from Egyptian deserts, are significantly higher compared to the activity concentrations for the investigated radionuclides reported in the literature from various countries around the world as shown in Table 1.

The analysis of Table 1 shows that the mean activity concentration of ^{226}Ra, ^{232}Th and ^{40}K in all studied samples are found to be 18508.49 ± 148.93, 9614.53 ± 27.94 and 2469.35 ± 75.72 Bq·kg^{-1}, respectively. These values are higher than world average radioactivity levels for building materials which are 35, 30 and 400 Bq·kg^{-1}, respectively [23].

In the sedimentary rock samples, the activity concentrations of ^{226}Ra ranged between 194.03 ± 3.32 (10H) and 142245.40 ± 1982.97 (9H) Bq·kg^{-1} with mean value of 31790.01 ± 247.60 Bq·kg^{-1}, while the concentration of ^{232}Th ranged between 10.33 ± 0.85 (2H) and 1842.86 ± 143.86 (9H) Bq·kg^{-1} with mean value of 225.73 ± 17.34 Bq·kg^{-1}. Finally, activity concentrations of ^{40}K varied between 100.15 ± 4.38 (7H) and 21733.77 ± 916.25 (9H) Bq·kg^{-1} with mean value of 2482.65 ± 108.79 Bq·kg^{-1}.

In the igneous rock samples in the one found that ^{226}Ra activity concentrations varied between 140.06 ± 2.82 (13H) and 22263.65 ± 38.99 (16H) Bq·kg^{-1} with mean value of 5125.7 ± 15.72 Bq·kg^{-1}. The highest value of ^{232}Th is 9278.23 ± 10.6 (18H) Bq·kg^{-1} and the lowest value found to be 106.08 ± 1.08 (13H) Bq·kg^{-1} and the mean value is 4041.04 ± 5.88 Bq·kg^{-1}. As for ^{40}K the activity concentrations ranged between 298.35 ± 4.26 (17H) and 2052.18 ± 18.31 (18H) Bq·kg^{-1} with mean value of 1447.87 ± 11.87 Bq·kg^{-1}.

In sediments samples, the ^{226}Ra activity concentration ranges between 6143.89 ± 155.16 (21H) and 10163.53 ± 210.93 (20H) Bq·kg^{-1} with mean value of 8153.71 ± 183.05 Bq·kg^{-1} while, the activity concentration of ^{232}Th ranges between 41878.96 ± 97.31 (21H) and 115234.3 ± 203.11 (20H) Bq·kg^{-1} with mean value of 78556.68 ± 150.21 Bq·kg^{-1} and ^{40}K activity concentration ranges between 3698.3 ± 112.41 (21H) and 9582.31 ± 175.88 (20H) Bq·kg^{-1} with mean value of 6640.31 ± 144.15 Bq·kg^{-1}.

The activity concentration of ^{226}Ra in conglomerate rock samples, is below the detection limit in sample (12H) and 82.39 ± 17.15 Bq·kg^{-1} in sample (11H), while ^{232}Th activity concentration ranges between 4037.15 ± 39.56 and 4632.68 ± 43.86 with mean value of 4334.92 ± 41.71 Bq·kg^{-1}. ^{40}K activity concentration ranges between 874.94 ± 47.46 and 1144.82 ± 55.17 Bq·kg^{-1} with mean value of 1009.88 ± 51.32 Bq·kg^{-1}. The highest value of ^{226}Ra activity concentrations was found in the sedimentary rock samples (9H) while the lowest activity concentrations of ^{226}Ra was found in the conglomerate rock samples (12H). These results show that the location where sedimentary rocks had been collected are characterized by high concentration of ^{238}U and low concentration of ^{232}Th as concluded by [24].

Table 1. The specific activities (Bq·kg^{-1}) of ^{226}Ra, ^{232}Th and ^{40}K for the studied samples.

Sample	Sample type	^{226}Ra (Bq·kg^{-1})	^{232}Th (Bq·kg^{-1})	^{40}K (Bq·kg^{-1})
1H		63634.66 ± 117.03	67.26 ± 6.92	560.33 ± 34.83
2H		5462.52 ± 13.74	10.33 ± 0.85	118.83 ± 6.69
3H		41226.26 ± 115.78	58.31 ± 7.97	334.52 ± 32.72
4H		247.32 ± 2.74	59.46 ± 0.73	348.02 ± 3.75
5H		204.52 ± 2.66	47.43 ± 0.66	293.01 ± 3.41
6H		39478.03 ± 139.65	102.39 ± 7.34	882.00 ± 59.25
7H		6455.06 ± 14.68	16.35 ± 1.36	100.15 ± 4.38
8H		18752.33 ± 83.43	18.10 ± 3.00	142.43 ± 22.16
9H		142245.40 ± 1982.97	1842.86 ± 143.86	21733.77 ± 916.25
10H		194.03 ± 3.32	34.76 ± 0.71	313.47 ± 4.41
Mean	Sedimentary	31790.01 ± 247.60	225.73 ± 17.34	2482.65 ± 108.79
11H		82.39 ± 17.15**	4632.68 ± 43.86	1144.82 ± 55.17
12H		---**	4037.15 ± 39.56	874.94 ± 47.46
Mean	Conglomerate	82.39 ± 17.15	4334.92 ± 41.71	1009.88 ± 51.32
13H		140.06 ± 2.82	106.08 ± 1.08	1501.88 ± 8.23
14H		1498.50 ± 13.71	8740.40 ± 8.37	1880.67 ± 12.20
15H		1679.59 ± 11.52	5668.61 ± 6.80	1724.92 ± 10.94
16H		22263.65 ± 38.99	1753.61 ± 6.72	2003.49 ± 19.74
17H		698.70 ± 5.77	587.54 ± 2.09	298.35 ± 4.26
18H		7761.36 ± 25.36	9278.23 ± 10.60	2052.18 ± 18.31
19H		1838.03 ± 11.88	2152.81 ± 5.48	673.61 ± 9.38
mean	Igneous	5125.7 ± 15.72	4041.04 ± 5.88	1447.87 ± 11.87
20H		10163.53 ± 210.93	115234.39 ± 203.11	9582.31 ± 175.88
21H		6143.89 ± 155.16	41878.96 ± 97.31	3698.30 ± 112.41
Mean	Sediments	8153.71 ± 183.05	78556.68 ± 150.21	6640.31 ± 144.15
	Greek[25]	74	85	881
	India [26]	25.88	42.82	560.6
	Iran [27]	77.4	44.5	1017.2
	Jordan [28]	41.5	58.4	897
	Nigeria[29]	63.29	226.6	832.5
Previous works	Palestine [30]	71	82	780
	Spain [31]	84	42	1138
	S. Arbia [32]	28.8	34.8	665.08
	Turkey [33]	80	101	974
	Egypt [22]	137	82	1082
	Egypt [21]	13176.00	11883.00	1573.00
	Present study	18508.49 ± 148.93	9614.53 ± 27.94	2469.35 ± 75.72

**Below the detection limits.

The obtained activity concentrations of ^{226}Ra, ^{232}Th and ^{40}K are used to calculate different hazards indices using Equations (2)-(10). The deduced values of D (nGy·h^{-1}), $AEDE$ in air (mSv·y^{-1}), Ra_{eq} (Bq Kg^{-1}), H_{ex}, H_{in}, I_{γ}, $AGDE$ (mSv·y^{-1}), $ELCR$ (mSv·y^{-1}) and ER (mR·h^{-1}) hazards indices are given in Table 2 compared to worldwide limits for building materials (WL).

In Figure 1 the absorbed dose rate (D) is plotted alongside the radium equivalent (Ra_{eq}) and exposure rate (ER) calculated for each sample. The results obtained reveal that the Ra_{eq} values for all samples exceed the permissible maximum value of 370 Bq·kg^{-1}, except for samples 4H, 5H, and 10H, which are sedimentary rocks. However, Table 3 presents the minimum, maximum, and mean values of (D), (Ra_{eq}), and (ER) for sedimentary, igneous, conglomerate, and sediments rock samples. It is evident from the table that the mean absorbed dose rate in sediments rocks is approximately three times greater than that in sedimentary

Table 2. The radiation hazards indices calculated for different samples.

| Sample No.	D (nGy·h^{-1})	$AEDE$ in air (mSv·y^{-1})	Ra_{eq} (Bq·kg^{-1})	H_{ex}	H_{in}	I_{γ}	$AGDE$ (mSv·y^{-1})	$ELCR$ (mSv·y^{-1})	ER (mR/h)
1H	29463.20	36.13	63773.84	172.36	344.35	425.28	197.09	119.24	121.25
2H	2534.88	3.11	5486.42	14.83	29.59	36.60	16.96	10.26	10.44
3H	19095.70	23.42	41335.29	111.72	223.14	275.65	127.74	77.28	78.57
4H	164.69	0.20	359.03	0.97	1.64	2.48	1.12	0.67	0.71
5H	135.36	0.17	294.82	0.80	1.35	2.03	0.92	0.55	0.59
6H	18337.47	22.49	39692.14	107.28	213.97	264.80	122.69	74.21	75.52
7H	2996.29	3.67	6486.12	17.53	34.98	43.26	20.05	12.13	12.33
8H	8680.45	10.65	18789.14	50.78	101.46	125.29	58.07	35.13	35.72
9H	67736.76	83.07	146549.89	396.08	780.53	981.22	454.07	274.14	281.29
10H	123.71	0.15	267.80	0.72	1.25	1.85	0.84	0.50	0.54
11H	2883.94	3.54	6788.57	18.35	18.57	47.64	19.98	11.67	11.08
12H	2474.92	3.04	5834.66	15.77	15.77	40.95	17.15	10.02	9.48
13H	191.41	0.23	407.13	1.10	1.48	3.00	1.35	0.77	0.98
14H	6049.93	7.42	14129.45	38.19	42.24	98.65	41.76	24.48	23.37
15H	4271.74	5.24	9910.29	26.78	31.32	69.03	29.43	17.29	16.66
16H	11428.53	14.02	24922.92	67.36	127.53	167.30	76.76	46.25	46.93
17H	690.12	0.85	1561.00	4.22	6.11	10.73	4.71	2.79	2.76
18H	9275.38	11.38	21173.84	57.23	78.20	145.89	63.41	37.54	36.55
19H	2177.55	2.67	4965.28	13.42	18.39	34.23	14.89	8.81	8.61
20H	74696.71	91.61	175521.19	474.38	501.85	1226.49	516.10	302.31	285.05
21H	28287.59	34.69	66255.46	179.07	195.67	462.21	195.2	114.48	108.32
(WL)	59	20	370	1	1	1	0.298	2.9E-4	0.600
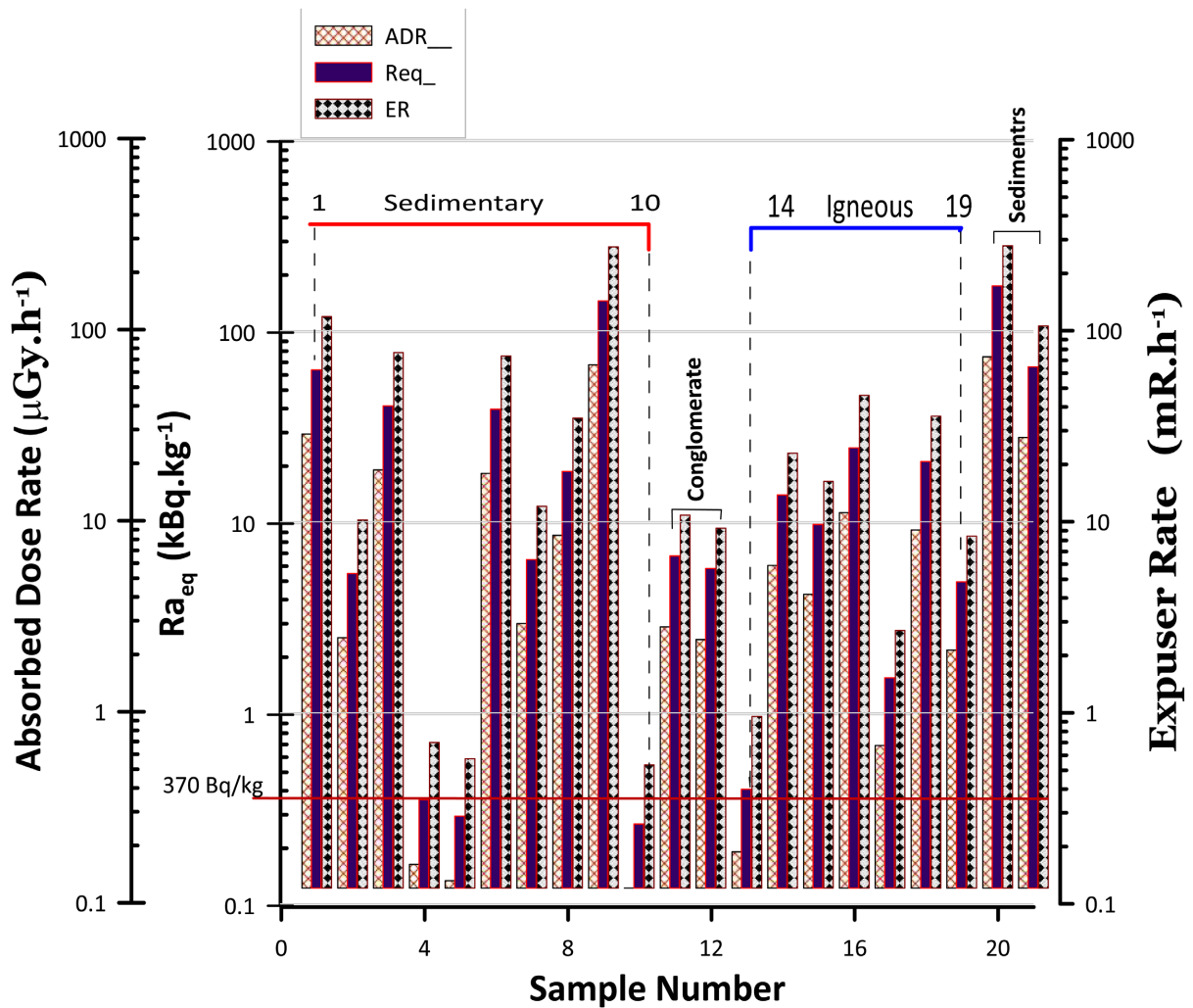
Figure 1. Variation of the absorbed dose rate, radium equivalent and exposure rate with sample number.

Table 3. Minimum, maximum, and mean value of the absorbed dose, radium equivalent and exposure rate in sedimentary (I), igneous (II), conglomerate (III) and sediments (IV) rocks.

Sample type	D (µGy/h)			Ra_{eq} (k Bq·kg^{-1})			ER (mR/h)		
	min	max	mean	min	max	mean	min	max	mean
I	0.16	67.74	16.57	0.27	146.55	32.30	0.55	281.29	61.69
II	0.19	11.43	4.87	1.56	24.92	12.78	2.76	46.93	22.48
III	2.47	2.88	2.68	5.83	6.79	6.31	9.48	11.08	10.28
IV	28.29	74.69	51.49	66.23	175.52	120.89	108.32	285.05	196.69

rocks, surpassing that in igneous rocks by a factor of 10.6, and exceeding that in conglomerate rocks by 19.2 times. The variation of the mean value of Ra_{eq} and exposure rate for each group of sample's number is shown in **Figure 2**.

One can conclude that sediments rocks contain high concentration of Th and U causes much more hazards effect than the igneous rocks which is trich in Th and sedimentary rocks which is rich in U. However, the conglomerate rock sam-

ples show the lowest hazards effect among all the tested samples.

In Table 4, the mean values of H_{in}, H_{ex}, and *AEDE* are provided for each category of rocks while, Figure 3 illustrates the variation of the mean values of H_{in}, H_{ex} and *AEDE* for sedimentary, igneous, conglomerate and sediments groups of rock's type. Analysis of the data reveals that the values of H_{ex} for samples 4H, 5H, and 10H (sedimentary rock), as well as sample 13H (igneous rock), fall within the permissible value of 1. However, it is noteworthy that H_{ex} exceeds the permissible limit for all other samples, indicating significant variations in radiation levels across the different rock categories.

In Figure 4, a linear relationship is depicted between the annual gonadal dose equivalent, excess lifetime cancer risk, radiation level index, and annual effective dose. The linearity coefficients corresponding to these relationships are determined to be 5.555, 12.651, and 3.3, respectively. From Equation 9, the risk factor (*RF*) can be inferred from the slope of the excess lifetime cancer risk (*ELCR*) line, yielding a value of 0.05, assuming a lifespan (*LF*) of 66 years, which is consistent with previous findings [19].
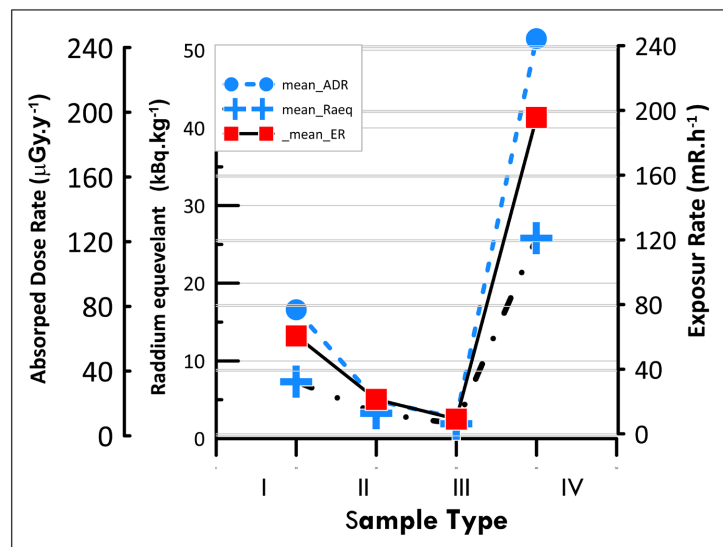

Figure 2. Variation of the mean value of the absorbed dose, radium equivalent and exposure rate in sedimentary (I), igneous (II), conglomerate (III) and sediments (IV) rocks.

Table 4. Minimum, maximum, and mean value of the internal, external hazard index and annual effective dose equivalent for sedimentary (I), igneous (II), conglomerate (III) and sediments (IV) rocks.

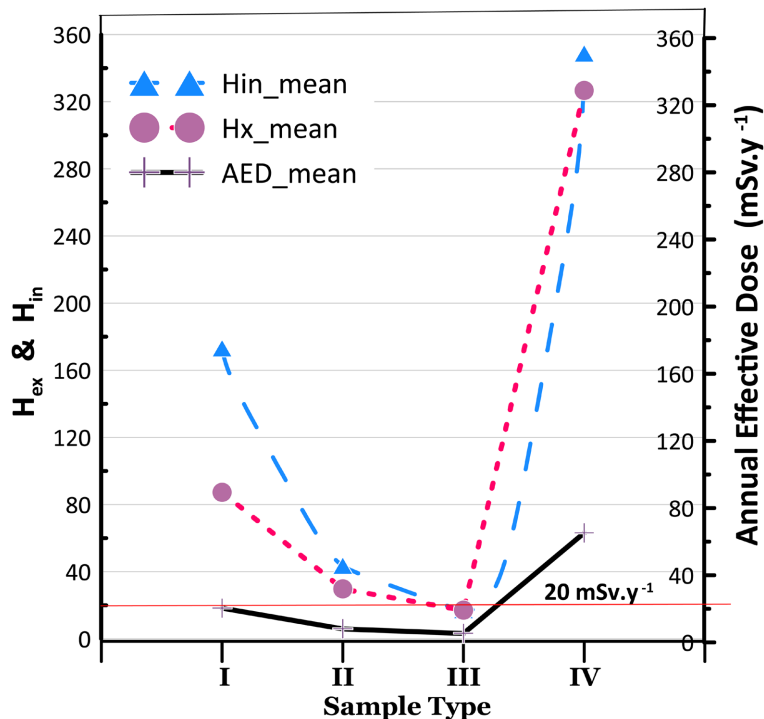| Sample Type	H_{in}			H_{ex}			*AEDE* (mSv/y)		
	min	max	mean	min	max	mean	min	max	mean
I	1.25	780.52	173.22	0.73	396.08	87.31	0.15	83.07	18.30
II	1.47	127.53	43.61	1.10	67.36	29.75	0.23	14.01	5.97
III	15.75	18.65	17.17	15.77	18.34	17.06	3.04	3.53	3.28
IV	195.67	501.85	348.76	179.07	474.38	326.73	34.69	91.60	63.14

Figure 3. Variation of the mean value of internal, external hazard index and annual effective dose equivalent in sedimentary (I), igneous (II), conglomerate (III) and sediments (IV) rocks.
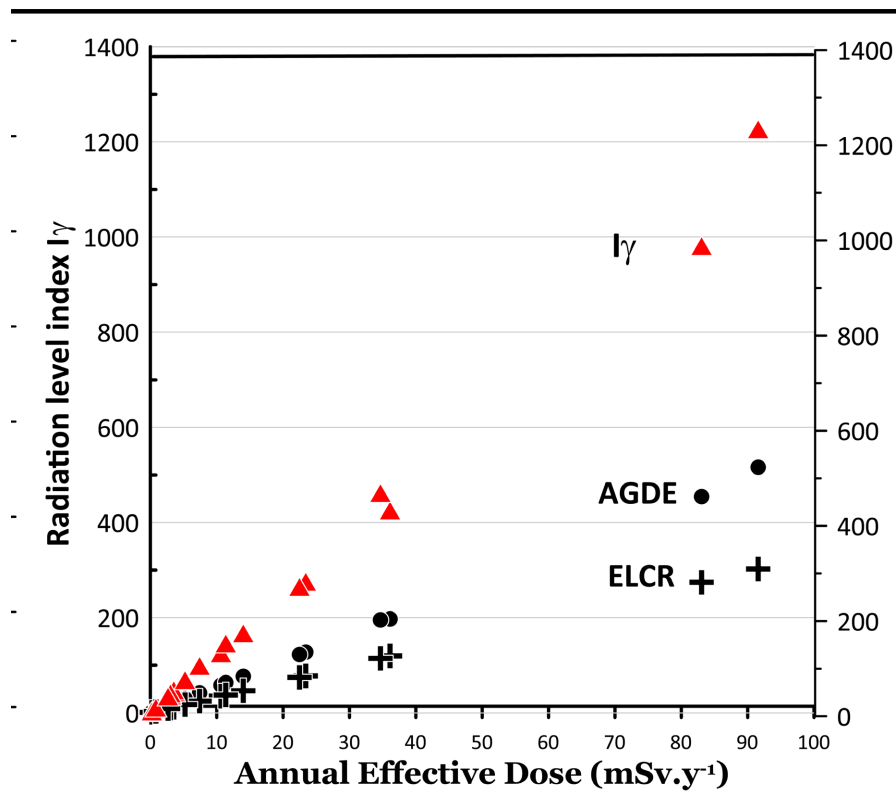

Figure 4. The mean value of annual gonadal dose, radiation level index and excess lifetime cancer risk with annual effective dose.

4. Conclusion

Twenty-one rock samples, including sedimentary, igneous, conglomerate, and sediments were collected from four distinct locations in Egypt's Eastern desert. Utilizing a high-performance gamma spectrometer equipped with a 100% efficiency hyper pure germanium detector, electric cooling, digital electronic systems, and a 16 k channels Multi-Channel Analyzer (MCA), specific activity concentrations of ^{226}Ra, ^{232}Th, and ^{40}K were measured. Results revealed heightened levels of ^{226}Ra in regions where sedimentary samples were obtained, whereas igneous samples exhibited a relatively higher concentration of ^{232}Th compared to ^{226}Ra. Sediments rock samples displayed elevated concentrations of both ^{232}Th and ^{226}Ra. Conversely, conglomerate rocks demonstrated low levels of radioactivity, particularly in ^{226}Ra. These findings align with previously published data on pegmatite rocks in Egypt. Comparative analyses were conducted with previously published international literature, providing valuable insights into the natural radioactivity variations across diverse geological formations and geographical regions. The comparisons contribute to a comprehensive understanding of radiation exposure risks pertinent to specific rock types and locations. Furthermore, hazard indices associated with most rock samples exceeded international safety standards, highlighting the significant radiation hazards inherent in the studied regions.

Conflicts of Interest

The authors declare no conflicts of interest regarding the publication of this paper.

References

[1] UNSCEAR (2000) Sources and Effects of Ionizing Radiation. Report to General Assembly, with Scientific Annexes, United Nations, New York.

[2] Bello, I.A., Jibiri, N.N. and Momoh, H.A. (2014) Determination of External and Internal Hazard Indices from Naturally Occurring Radionuclide in Rock, Sediment and Building Samples Collected from Sikiti, Southwestern Nigeria. *Journal of Natural Sciences Research*, **4**, 744-781.

[3] Khatun, M.A., Ferdous, J. and Haque, M.M. (2018) Natural Radioactivity Measurement and Assessment of Radiological Hazards in Some Building Materials Used in Bangladesh. *Journal of Environmental Protection*, **9**, 1034-1048.
https://doi.org/10.4236/jep.2018.910064

[4] Itodo, A.U., Edimeh, P.O., Eneji, I.S. and Wuana, R.A. (2020) Radiological Impact Assessment of Mining on Soil, Water and Plant Samples from Okobo Coal Field, Nigeria. *Journal of Geoscience and Environment Protection*, **8**, 65-81.
https://doi.org/10.4236/gep.2020.85005

[5] Al-Jundi, J. (2002) Population Doses from Terrestrial Gamma Exposure in Areas Near to Old Phosphate Mine, Russaifa, Jordan. *Radiation Measurements*, **35**, 23-28.
https://doi.org/10.1016/S1350-4487(01)00261-X

[6] γ Vision A66-BW Software (2015) User's Manual γ-Ray Spectrum Analysis and MCA·Emulator for Microsoft Windows.

[7] Purnama, D.S. and Akbari, M.K. (2020) Validation and Calibration of Efficiency of Various Standard Source for Radioactivity Analysis of γ Soil Samples. I*Journal of*

Physics: Conference Series, **1436**, Article ID: 012059.
https://doi.org/10.1088/1742-6596/1436/1/012059

[8] Maurice, O.M. (2018) Modeling a HPGe Detector's Absolute Efficiency as a Function of γ Energy and Soil Density in Uncontaminated Soil. *SDRP Journal of Earth Sciences & Environmental Studies*, **3**, 1-6.

[9] Al-Tuweity, J., Kamleh, H., Al-Masri, M.S., Doubal, A.W. and Chakir, E. (2021) Self-Absorption Correction Factors: Applying a Simplified Method to Analysis of Lead-210 in Different Environment Samples by Direct Counting of Low-Energy Using HPGe Detector. *E3S Web of Conferences*, **240**, Article ID: 03002.
https://doi.org/10.1051/e3sconf/202124003002

[10] Ehsan, S., *et al.* (2019) The Activity Concentration of Radionuclides (226ra, 232th and 40k) in Soil Samples and Associated Health Hazards in Natore, Kushtia and Pabna District of Bangladesh. *Journal of Bangladesh Academy of Sciences*, **43**, 169-180. https://doi.org/10.3329/jbas.v43i2.45738

[11] Al-Zahrani, B.M., Alqannas, H.S. and Hamidalddin, S.H. (2020) Study and Simulated the Natural Radioactivity (NORM) U-238, Th-232 and K-40 of Igneous and Sedimentary Rocks of Al-Atawilah (Al-Baha) in Saudi Arabia. *World Journal of Nuclear Science and Technology*, **10**, 171-181.
https://doi.org/10.4236/wjnst.2020.104015

[12] Ngachin, M., Garavaglia, M., Giovani, C., Kwato Njock, M.G. and Nourreddine, A. (2007) Assessment of Natural Radioactivity and Associated Radiation Hazards in Some Cameroonian Building Materials. *Radiation Measurements*, **42**, 61-67.
https://doi.org/10.1016/j.radmeas.2006.07.007

[13] Arafa, W. (2004) Specific Activity and Hazards of Granite Samples Collected from the Eastern Desert of Egypt. *Journal of Environmental Radioactivity*, **75**, 315-327.
https://doi.org/10.1016/j.jenvrad.2004.01.004

[14] Abdel-Rahman, M.A.E. and El-Mongy, S.A. (2017) Analysis of Radioactivity Levels and Hazard Assessment of Black Sand Samples from Rashid Area, Egypt. *Nuclear Engineering and Technology*, **49**, 1752-1757.
https://doi.org/10.1016/j.net.2017.07.020

[15] Nada, A. (2004) γ Spectroscopic Analysis for Estimation of Natural Radioactivity Levels in Some Granite Rocks of Eastern Desert, Egypt. *Arab Journal of Nuclear Science and Application*, **37**, 201-222.

[16] El-Hussein, A. (2005) A Study on Natural Radiation Exposure in Different Realistic Living Rooms. *Journal of Environmental Radioactivity*, **79**, 355-367.
https://doi.org/10.1016/j.jenvrad.2004.08.009

[17] Diab, H.M., Nouh, S.A., Hamdy, A. and El-Fiki, S.A. (2008) Evaluation of Natural Radioactivity in a Cultivated Area around a Fertilizer Factory. *Journal of Nuclear Radiation Physics*, **3**, 53-62.

[18] Bassioni, G., Abdulla, F., Morsy, Z. and El-Faramawy, N. (2012) Evaluation of Naturally Occurring Radioactive Materials (NORMs) in Inorganic and Organic Oilfield Scales from the Middle East. *Archives of Environmental Contamination and Toxicology*, **62**, 361-368. https://doi.org/10.1007/s00244-011-9706-7

[19] Taskin, H., Karavus, M., Ay, P., Topuzoğlu, A., Hidiroglu, S. and Karahan, G. (2008) Radionuclide Concentrations in Soil and Lifetime Cancer Risk Due to γ Radioactivity in Kirklareli, Turkey. *Journal of Environmental Radioactivity*, **100**, 49-53.
https://doi.org/10.1016/j.jenvrad.2008.10.012

[20] Darwish, D.A.E., Abul-Nasr, K.T.M. and El-Khayatt, A.M. (2015) The Assessment of Natural Radioactivity and Its Associated Radiological Hazards and Dose Para-

meters in Granite Samples from South Sinai, Egypt. *Journal of Radiation Research and Applied Sciences*, **8**, 17-25. https://doi.org/10.1016/j.jrras.2014.10.003

[21] Abd El Rahman, R.M., *et al.* (2022) Natural Radionuclide Levels and Radiological Hazards of Khour Abalea Mineralized Pegmatites, Southeastern Desert, Egypt. *Minerals*, **12**, Article 353. https://doi.org/10.3390/min12030353

[22] Amin, R.M. (2012) γ Radiation Measurements of Naturally Occurring Radioactive Samples from Commercial Egyptian Granites. *Environmental Earth Sciences*, **67**, 771-775. https://doi.org/10.1007/s12665-012-1538-x

[23] Michael, F., Parpottas, Y. and Tsertos, H. (2010) Gamma Radiation Measurements And Dose Rates in Commonly Used Building Materials in Cyprus. *Radiation Protection Dosimetry*, **142**, 282-291. https://doi.org/10.1093/rpd/ncq193

[24] Regelous, A., Scharfenberg, L. and De Wall, H. (2021) Origin of S-, A- and I-Type Granites: Petrogenetic Evidence from Whole Rock Th/U Ratio Variations. *Minerals*, **11**, Article 672. https://doi.org/10.3390/min11070672

[25] Papadopoulos, A., Christofides, G., Koroneos, A., Papadopoulou, L., Papastefanou, C. and Stoulos, S. (2013) Natural Radioactivity and Radiation Index of the Major Plutonic Bodies in Greece. *Journal of Environmental Radioactivity*, **124**, 227-238. https://doi.org/10.1016/j.jenvrad.2013.06.002

[26] Senthilkumar, G., Raghu, Y., Sivakumar, S., Chandrasekaran, A., Prem Anand, D. and Ravisankar, R. (2014) Natural Radioactivity Measurement and Evaluation of Radiological Hazards in Some Commercial Flooring Materials Used in Thiruvannamalai, Tamilnadu, India. *Journal of Radiation Research and Applied Sciences*, **7**, 116-122. https://doi.org/10.1016/j.jrras.2013.12.009

[27] Abbasi, A. (2013) Calculation of γ Radiation Dose Rate and Radon Concentration Due to Granites Used as Building Materials in Iran. *Radiation Protection Dosimetry*, **155**, 335-342. https://doi.org/10.1093/rpd/nct003

[28] Sharaf, J.M. and Hamideen, M.S. (2013) Measurement of Natural Radioactivity in Jordanian Building Materials and Their Contribution to the Public Indoor γ Dose Rate. *Applied Radiation and Isotopes*, **80**, 61-66. https://doi.org/10.1016/j.apradiso.2013.06.016

[29] Akpanowo, M.A., Umaru, I., Iyakwari, S., Joshua, E.O., Yusuf, S. and Ekong, G.B. (2020) Determination of Natural Radioactivity Levels and Radiological Hazards in Environmental Samples from Artisanal Mining Sites of Anka, North-West Nigeria. *Scientific African*, **10**, e00561. https://doi.org/10.1016/j.sciaf.2020.e00561

[30] Thabayneh, K.M. (2013) Measurement of Natural Radioactivity and Radon Exhalation Rate in Granite Samples Used in Palestinian Buildings. *Arabian Journal for Science and Engineering*, **38**, 201-207. https://doi.org/10.1007/s13369-012-0391-2

[31] Guillén, J., Tejado, J.J., Baeza, A., Corbacho, J.A. and Muñoz, J.G. (2014) Assessment of Radiological Hazard of Commercial Granites from Extremadura (Spain). *Journal of Environmental Radioactivity*, **132**, 81-88. https://doi.org/10.1016/j.jenvrad.2014.02.004

[32] AlZahrani, J.H., Alharbi, W.R. and Abbady, A.G.E. (2011) Radiological Impacts of Natural Radioactivity and Heat Generation by Radioactive Decay of Phosphorite Deposits from Northwestern Saudi Arabia. *Australian Journal of Basic and Applied Sciences*, **5**, 683-690.

[33] Aykami, S.A., Turhan, S., Aysun Ugur, F., Baykan, U.N. and Kiliç, A.M. (2013) Natural Radioactivity, Radon Exhalation Rates and Indoor Radon Concentration of Some Granite Samples Used as Construction Material in Turkey. *Radiation Protection Dosimetry*, **157**, 105-111. https://doi.org/10.1093/rpd/nct110